Petrology and Geochemistry of the Metasediments of the Janub Metamorphic Suite, Southern Jordan: Implications for Geothermobarometry and Economic Potential

Mahmoud A. Habboush [a,*], Ghaleb H. Jarrar [b]

[a]Department of Supervision, Ministry of Education, Amman, Jordan.

[b]Department of Environmental and Applied Geology, University of Jordan, 11942 Amman, Jordan

Abstract

Petrographical and geochemical characteristics of the hornfelses and metaconglomerates of the Janub metamorphic suite have been examined to reveal their geothermobarometry and economic potential. The temperature of metamorphism attained by hornfelses ranges between 500°C and 545 °C with an average temperature of 522°C, while metaconglomerate may show a wider range between 300 °C to 600 °C with an average temperature 520 °C. Mineralogy of the metasediments indicates a low pressure type of metamorphism (< 4 Kbar). These conditions correspond to metamorphism equivalent to upper greenschist to lower amphibolite facies. The identified opaque minerals are ilmenite, magnetite and titanomagnetite. Sulphides are less abundantand include pyrite, cinnabar, pyrrhotite, sphalerite, galena and chalcopyrite.

1. Introduction

The Precambrian basement complex of Jordan is located at the northernmost extremity of the Arabian-Nubian Shield (ANS). The formation of ANS took place mainly during the Pan-African Orogeny 900-550Ma; (Kröner, 1985). This basement consists of igneous, sedimentary and metamorphic rocks; and is exclusively of Neoproterozoic age 550-800 Ma (e.g., Jarrar et al., 2003). These rocks are broadly divided into two broad lithostratigraphic divisions: the Aqaba and Araba complexes (McCourt & Ibrahim, 1990). The Janub Metamorphic Suite (JMS), which belongs to the Aqaba Complex, is the theme of this study (Fig. 1).

The study area is located in the southernmost corner of Jordan near the Jordan –Saudi Arabia border. The JMS is considered as one of the oldest suites together with Abu Barqa metasedimentary suite. McCourt & Ibrahim (1990) described Janub suite rocks as low grade metamorphic rocks, belonging to lower – middle greenschist facies. Characteristically, these are preserved as roof pendants and large xenoliths in Abu Jedda monzogranite (Yutum suite). Most lithologies in this area are metasediments dipping to the north with an approximate E-W directed strike. Hassuneh (1994) divided the metasedimentary rocks in this area on the basis of petrographical and geochemical criteria into three groups:

a. Cordierite – biotite hornfels
b. Metaconglomerates.
c. Quartzo – feldspathic metasediments.

This study aims at revealing conditions of formation in terms of pressure, temperature, and the mineralogy and geochemistry of the opaque minerals to evaluate their economic potential

2. Analytical Techniques

The investigated rocks were analyzed using Inductively Coupled Plasma Mass Spectroscopy (ICP-MS) at the Institute für Geowissenschaften of the Technical University of Braunschweig, Germany for their major, minor, and trace elements. The Mineral separation was carried out at the Geology Department, University of Jordan.

Mineral analyses have been carried out by the third author on the Cameca SX100 microprobe at the Institute of Mineralogy, University of Stuttgart, Germany

3. Petrography

The first detailed petrographical description of Janub metamorphic suite was carried out by Rabba and Ibrahim (1988) and Hassuneh (1994). In the present study only two rock types were studied: namely hornfelses and metaconglomerates.

3.1. Pelitic Hornfelses

The investigated hornfelses are composed of biotite and quartz as major minerals and subordinate cordierite, sillimanite, K-feldspar, and amphibole. Chlorite occurs as

---
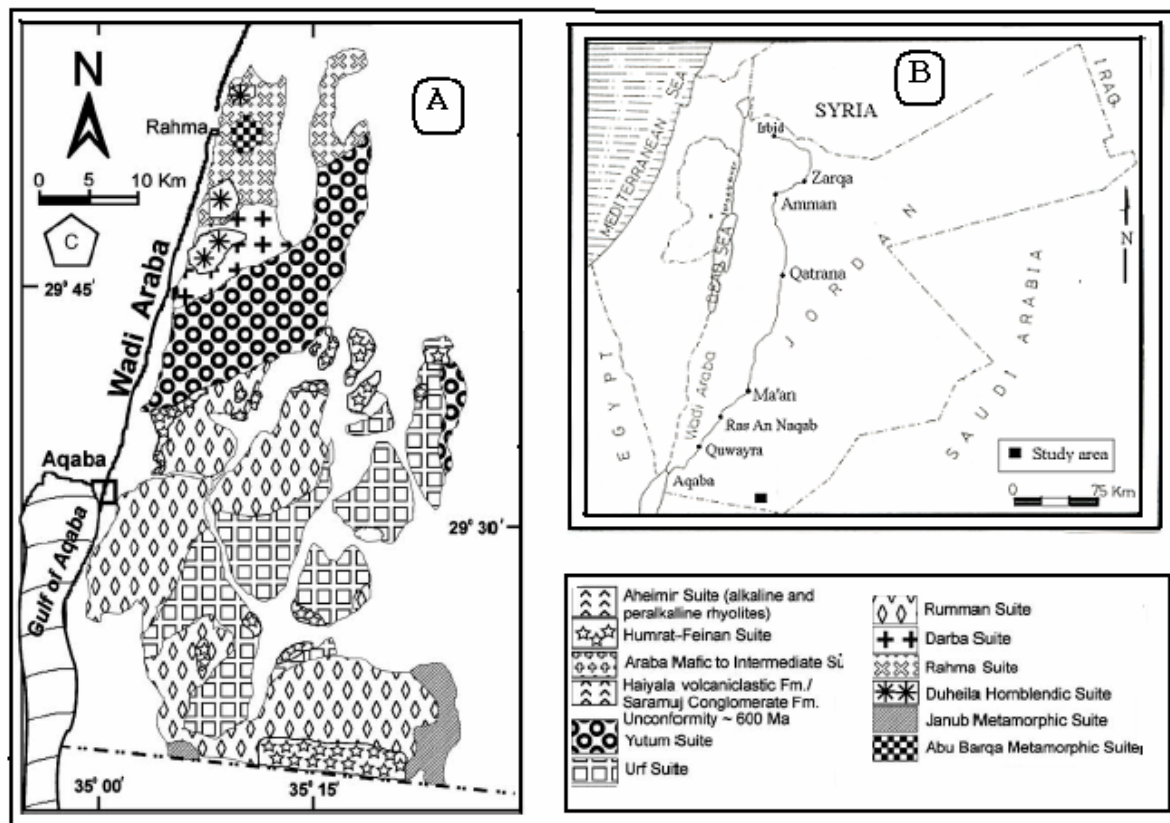* Corresponding author. habboush_m@yahoo.com

Figure 1. A. Location map of the principal suites of Aqaba Complex (after Jarrar et al., 2003), B. Location map showing the study area..

pseudomorphs after biotite. Accessory minerals are opaques and corundum.

The investigated rocks are characterized by preservation of some original sedimentary textures such as quartz granules and pebbles, phenocrysts and bedding planes. These features imply a lack of intense deformation during contact metamorphism (Hyndman, 1985).

Decussate texture (Fig. 2), Poikiloblastic and sieve textures (Fig. 3) are the most commonly encountered textures in hornfelses.

Most of the cordierite porphyroblasts in thin sections are anhedral, which together with the numerous inclusions indicate a rapid growth (Barker, 1990).

The occurrence of cordierite in Mg – rich rocks (low Fe /Fe+Mg ratio) of the bulk composition of hornfelses indicate low pressure and low water content (Yardly, 1989). Cordierite may form at low pressure in pelitic rocks according to the following reaction:

Chlorite + Muscovite → Cordierite + Biotite +Quartz + H_2O (Hyndman, 1985)
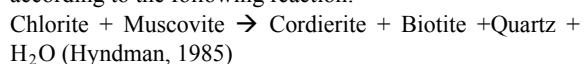
3.2. Metaconglomerates

The mineralogy of the metaconglomerates varies as a function of their original mineral content and texture since they were derived from different sources. The coarse-grained varieties of these rocks are mainly of quartzo-feldspathic, granitoidal and arkosic lithologies, with grain size ranging between 2mm to 10mm. The dominant minerals in these rocks are quartz, biotite, K-feldspar, plagioclase, amphibole, chlorite and opaques. Minor minerals include: epidote, muscovite, secondary clay minerals, garnet and tourmaline.

Granoblastic (Fig 4), poikiloblastic, and cataclastic textures are very common. The latter is characterized by wavy extinction, mortar textures, fracturing, and elongated grains (Fig 5). Furthermore, most of the samples consist of quartz, K-feldspar, plagioclase, biotite, chlorite pseudomorphs after biotite, amphibole and opaques. According to Hassuneh (1994) this mineral assemblage is characteristic for quartzo-feldspathic rocks.

In the two metasedimentary lithologies, the opaques vary in size (0.01 up to 0.25mm), while in the metaconglomerates they occur as small grains distributed in the whole sample or concentrated in vein-like aggregates; in hornfelses opaques are less abundant. In most of the samples the opaque granules are associated with mafic minerals.

4. Geochemistry

The chemical composition of the investigated rocks is presented in Tables (1) and (2).

Several plots have been used to reveal the petrological evolution of the suite and to help make inferences regarding the protolith of the metamorphic rocks. The metaconglomerates show a negative relationship between SiO_2 vs. MnO, Fe_2O_3, TiO_2, MgO, Al_2O_3, and CaO; a positive correlation between SiO_2 vs. K_2O, and a slightly positive correlation between Na_2O with SiO_2 (Fig 6). These trends reflect the relationships between the elements in the source rocks and/or the behaviour of elements during weathering.
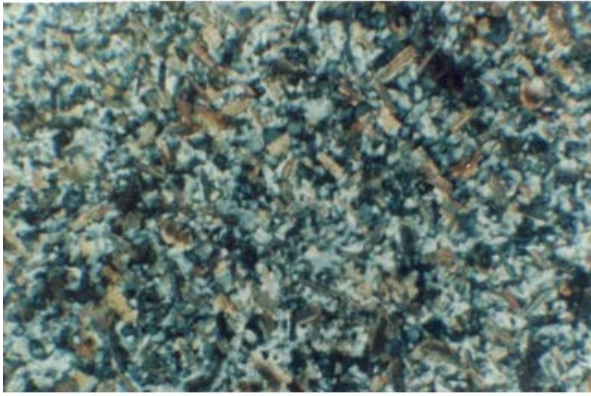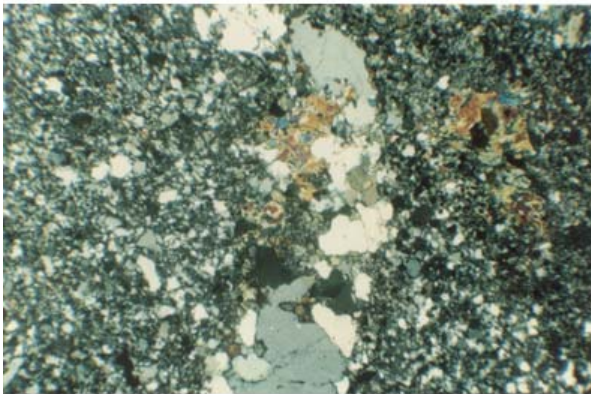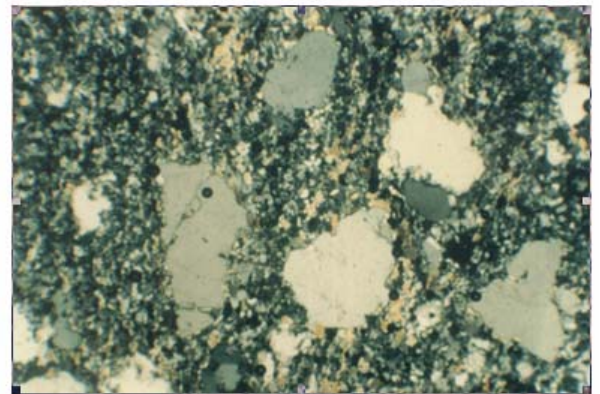
Fig. 2

Fig. 3

Fig. 4

Fig. 5.

Figures (2-5): Figure 2. Decussate texture: prismatic grains of biotite (brown) distributed randomly around quartz grains (white to gray). (Mag. 250, XPL), Figure 3. Cordierite porphyroblasts (at the center to the top right) with numerous inclusions of biotite forming sieve texture. (Mag. 125, XPL), Figure 4. Granoblastic quartz filling a vein, clots of small crystals of amphiboles can also be seen. Note the differences in the grain size of quartz. (Mag. 125, XPL) , Figure 5. Relics of large grains of quartz surrounded by small grains of amphibole, and quartz, note the fracturing of relic grains. (Mag. 50, XPL).

The resistant minerals such as quartz are retained as framework components while the other rock fragments of less resistive composition have gone into the matrix, therefore most of Fe_2O_3, MgO and CaO are in the matrix (Naqvi et al., 1988). The negative correlation of these oxides with SiO_2 supports this conclusion and reflects a decrease in the unstable component (e.g. rock fragments and feldspar) with an increase in mineralogical maturity (Gu et al., 2002). The positive correlation between K_2O vs. SiO_2 and scatter between on the Na_2O vs. SiO_2 diagram reflects the abundance of felsic rock fragments in the metaconglomerates.

The hornfelses display the same features as metaconglomerate with the exception of CaO (Fig (7). The positive correlation of CaO with SiO_2 reflects the preference of CaO to reside in the fine-grained matrix during sedimentary processing (Naqvi et al. 1988). The high negative correlation between SiO_2 with other major elements reflects similarity of the matrix in sedimentary rocks such as greywackes. (Naqvi et al., 1988). Saupe and Vegas (1987) have used the K/Al vs. Na/Al and (Fe+Mg)/ (Al/Na) vs. K/(Al-Na) to classify clastic sedimentary rocks into shale, greywacke and arkoses. The hornfelses fall in the shale field while the most of metaconglomerates fall in greywacke and to a lesser degree in arkoses field (Fig. 8).

5. Mineral Chemistry

Mineral chemistry is used to constrain P – T conditions of metamorphism and shed light on the origin of the protolith of the investigated rocks. The chemical data of the analyzed minerals are presented in Tables 2 to 6.

5.1. Pyroxenes

The pyroxenes are essential minerals in most mafic to ultramafic igneous rocks and high-grade metamorphic rocks. Pyroxene classification scheme after Morimoto et al., (1988) has been used to divide the analyzed pyroxenes into:
- Ferroan diopside; and
- Sub calcic magnesium rich augite. Table (2).

Clinopyroxenes appear only in some samples of the metaconglomerate.
$X_{Mg} = Mg/(Mg + \sum Fe$ of pyroxenes ranges between (44.9 − 73.7) with average of 63.7; and the (Wo) content ranges between 26.7 and 46.9.

5.2. Feldspars

Feldspars are the most abundant mineral group in the Earth's crust and form about 50% by weight of both continental and oceanic crust. The compositional triangle of feldspars has been used to divide the analyzed plagioclase into oligoclase and andesine. Plagioclase in metamorphic rocks becomes anorthite-rich with increasing

Table 1. Major (in wt %) and trace (in ppm) elements concentrations and elements ratios for the metaconglomerate and the hornfelses rocks.

Sample	A1	A5	A7	A8	A9	A10	A11	A12	A13	A14	A20	A22	A24	A30	A31	A38	A40	Z28	Z29	Z30	Z31	Z32	Z33	54x
SiO_2	64.2	66.74	72.14	64.05	64.2	60.27	71.62	65.22	62.5	67.03	69.05	56.9	66.48	63.89	60.29	70.61	66.52	64.62	58.42	58.51	58.5	64.28	62.36	60.91
Al_2O_3	14.32	15.16	13.45	14.81	13.26	16.27	14.07	15.68	15.33	14.43	14.84	18.46	13.89	14.45	15.75	13.94	16.35	15.2	14.51	13.86	15.93	14.5	15.87	15.65
Fe_2O_3	2.89	3.35	1.98	6.06	5.16	7.16	2.68	5.42	5.35	4.97	2.32	5.57	3.59	6.8	7.87	1.34	6.39	6.05	7	6.16	6.69	5.76	6.79	7.8
MgO	1.4	1.48	0.46	1.48	0.97	2.71	0.71	2.43	1.73	1.34	1.04	2.5	2.24	2.61	2.33	0.29	2.63	2.48	2.92	2.62	2.8	2.38	2.88	3.55
MnO	0.06	0.08	0.08	0.16	0.23	0.15	0.08	0.07	0.06	0.06	0.06	0.09	0.08	0.08	0.21	0.02	0.08	0.11	0.1	0.12	0.09	0.09	0.14	0.17
CaO	1.58	2.92	2.41	4.25	6.54	3.32	2.61	3.96	3.82	3.35	2.98	4.16	2.11	2.22	1.69	0.36	1.61	0.94	1.21	1.4	2.17	1.8	1.08	1.84
TiO_2	0.55	0.43	0.39	0.97	0.45	1.26	0.43	0.61	0.69	0.64	0.4	0.76	0.66	0.97	1.06	0.28	0.79	0.74	0.76	0.79	0.84	0.7	0.83	0.77
Na_2O	3.3	4.11	2.62	4.18	1.99	2.78	2.8	3.49	3.73	3.14	3.25	4	3.77	3.51	4.07	4.41	2.77	1.99	2.29	2.31	3.43	2.43	2.2	2.13
K_2O	4.12	1.58	3.64	2.44	2.67	3.71	3.47	2.24	2.88	2.32	2.58	2.17	4.09	3.67	4.23	5.02	2.63	2.91	2.54	2.58	2.41	2.17	2.23	1.79
P_2O_5	0.17	0.09	0.11	0.26	0.16	0.29	0.12	0.12	0.14	0.17	0.07	0.29	0.17	0.22	0.26	0.03	0.15	0.17	0.17	0.18	0.28	0.52	0.19	0.16
Total	92.6	95.94	97.27	98.66	95.63	97.91	98.59	99.23	96.22	97.44	96.57	94.91	97.07	98.42	97.76	96.31	99.93	95.22	89.93	88.53	93.14	94.64	94.56	94.78
Trace elements (ppm)																								
Ba	1400	770	2041	572	1379	1249	1197	826	1004	302	1416	517	1068	818	627	778	453	663	448	532	631	554	631	423
Th	11	9	10	5	9	7	9	5	6	4	12	5	12	6	8	12	5	5	5	5	6	6	6	6
U	5	2	3	2	4	2	3	2	2	2	4	2	4	2	3	4	2	2	1	2	2	2	2	2
Nd	37	47	50	32	48	44	53	22	28	22	31	21	30	31	46	35	25	25	23	26	31	39	28	27
Sm	7	10	10	7	10	9	10	5	6	5	6	5	6	7	10	7	6	5	5	6	7	9	6	6
B	65	46	23	103	88	123	33	88	89	71	37	99	55	120	135	19	98	99	116	106	117	100	124	129
Cd	1	1	-2	2	0	3	-1	1	1	1	107	2	0	2	2	2	2	2	0	0	4	3	2	3
Cr	21	11	1	91	10	72	9	71	69	69	16	71	104	43	37	14	118	112	39	32	142	120	139	144
Cu	6	10	0	158	2	0	28	39	182	10	205	1	17	29	5	16	11	32	49	43	8	26	12	31
Ni	17	9	10	36	12	31	12	27	21	25	608	23	42	24	20	13	37	41	164	169	50	44	50	50
Pb	264	210	336	222	291	180	239	177	186	235	31	193	192	182	200	283	202	195	151	123	141	159	160	182
Sr	486	665	677	457	603	540	556	489	435	162	54	452	455	280	199	68	173	165	108	109	373	209	168	204
V	90	49	36	149	50	148	41	111	127	104	174	139	102	148	142	28	131	129	78	53	157	145	156	156
Zn	46	52	42	62	45	98	39	28	32	37	41	52	42	45	169	27	44	75	175	195	41	64	60	105
Zr	94	226	316	174	255	215	306	115	144	147	174	164	157	248	305	210	189	177	175	195	193	191	172	183

metamorphic grade (Laird and Albee, 1981). In sample (A9) the plagioclase is of labradorite (An= 50%) and anorthite (An=97%) composition. The plagioclase of this sample is most probably of relict igneous origin.

Barium in orthoclase ranges from zero to 0.81 wt. % with an average of 0.38 due to substitution of barium for potassium. The anorthite content of the plagioclase in hornfelses ranges from 27 – 32 % and in metaconglomerates from 1 to 34 %, with the exception of the above mentioned sample (A9). Table (3)

5.3. Mica

Micas are a major group of phyllosilicates, common in igneous, metamorphic, and sedimentary rocks. All micas in the samples with the exception of X51 are biotites. This sample was taken from a rhyolitic dyke and contains muscovite, table (4).

Biotite is iron-rich with X_{Mg} = (Mg/(Fe+Mg)) ranging from 29 to 48 and averaging 39 for all samples. Ti ranges between 0.05 – 5.93 wt. % with an average value of 3.03; and Ba ranges between 0 – 0.19 wt. percentage with an average value of 0.08. This indicates that most barium in

the samples was substituted for potassium in the feldspar rather than biotite. Al^{iv} and probably Al^{vi} and Ti increase in biotite with increasing metamorphic grade (Laird and Albee, 1981).

The X_{Mg} of the biotites in sample X54 ranges between 29 and 34, almost the same as the X_{Mg} of the whole rock for this sample, which implies that biotite is the only Mg-bearing mineral in this sample. On the other hand, the X_{Mg} of the whole rock of A9 = 16.2, while the X_{Mg} value of biotite in A9 equals 48.

The X_{Fe} ratio of biotite mainly depends on oxygen fugacity, therefore at elevated oxygen fugacity (f_{O2}), biotite becomes rich in Mg (Wones and Eugster, 1965). The elevated iron content of the biotite reflects low oxygen fugacity during their formation.

5.4. Titanite (CaTiSiO5)

This mineral is composed of (26.7 – 28.2%) CaO, (35.09 – 38.5%) TiO_2 and (30.2 – 31.1%) SiO_2 with minor amounts of Al, Fe, Mn, and Cr. Table (5)

Table 2: The chemical composition and formulae of pyroxenes.

Sample. No.	A9$_1$	A9$_2$	Hc$_5$
	Wt%	Wt%	Wt%
SiO$_2$	51.062	45.413	50.927
TiO$_2$	0.048	0.437	0.187
Al$_2$O$_3$	1.198	6.798	3.933
Cr$_2$O$_3$	0.029	0.021	0.017
FeO	8.706	15.197	10.059
MnO	1.879	1.512	0.970
MgO	12.336	12.390	16.563
CaO	21.719	11.849	12.516
Na$_2$O	0.163	0.703	0.494
K$_2$O	0.318	0.318	0.318
TOTAL	97.458	94.638	95.984
No Oxygens	6	6	6
Si	1.974	1.822	1.945
Al	0.026	0.178	0.055
Al	0.028	0.143	0.122
Fe(iii)	0.034	0.117	0
Cr	0.001	0.001	0.001
Ti	0.001	0.013	0.005
Fe(ii)	0.247	0.0388	0.322
Mn	0.062	0.051	0.031
Mg	0.711	0.741	0.943
Ca	0.899	0.509	0.512
Na	0.012	0.055	0.037
K	0.016	0.016	0.015
TOTAL	4.010	4.034	3.988
X Mg	58.6	44.9	62.2
Wo	45.78	27.36	27.76
En	36.18	39.82	51.1
Fs	17.41	29.88	19.16
Ac	0.62	2.94	1.98

Table 3: The chemical analyses and formulae for the feldspar. The formulae were calculated on the bases of 8 oxygen's.

Sample	X54	b	A9	X51	HC-M
Na$_2$O	8.65	6.20	6.58	0.59	1.56
SiO$_2$	58.35	58.23	59.48	44.82	65.91
Al$_2$O$_3$	24.44	27.40	24.73	34.11	18.81
MgO	0.00	0.02	0.44	0.37	0.01
K$_2$O	0.06	0.28	2.85	9.82	14.01
CaO	5.81	9.34	2.62	0.07	0.07
TiO$_2$	0.00	0.06	0.01	0.33	0.00
FeO	0.27	0.18	0.53	1.97	0.02
BaO	0.00	0.02	0.00	0.00	0.30
Summe	97.60	101.72	97.23	92.07	100.68
Na	0.768	0.530	0.584	0.057	0.138
Si	2.671	2.569	2.722	2.247	3.000
Al	1.318	1.425	1.334	2.016	1.009
Mg	0.000	0.001	0.030	0.028	0.001
K	0.004	0.016	0.166	0.628	0.814
Ca	0.285	0.442	0.128	0.004	0.003
Ti	0.000	0.002	0.000	0.012	0.000
Fe	0.010	0.006	0.020	0.082	0.001
Ba	0.000	0.000	0.000	0.000	0.005
Summe	5.056	4.991	4.984	5.074	4.971
Albite %	72.679	53.653	66.466	8.309	14.370
Orthoclase %	0.346	1.599	18.936	91.151	84.745
Anorthite %	26.975	44.715	14.596	0.529	0.335
Celsian %	0.000	0.033	0.002	0.011	HC-M

5.5. Opaques

Most of opaque phases in the analyzed samples are titanium and iron oxides and minor quantities of sulfides especially pyrite (Table 5)

5.5.1. Ilmenite (Fe Ti O$_3$)

Ilmenite is composed of (35.5 – 51.1%) TiO$_2$, (35.7 – 54.7%) FeO, (1.98 – 12.5) MnO, and minor amounts of Cr. The formula can be expressed as (Fe, Mg, Mn) TiO$_3$ with limited Mg and Mn substitution for iron

5.5.2. Pyrite (FeS2)

The iron content of pyrite in X51 sample ranges between 47.15 %– 49.66 % with an average value of 48.25 %. In general, pyrite is composed of 46.6 % Fe and 53.4 % S and minor amounts of Co, Ni. (Klein, 2002).

5.5.3. Magnetite

It is mostly composed of (88.7 – 93.5%) of total iron. Fe$_2$O$_3$ content ranges from 6.26 to 10.6%) and FeO content ranges from 79.6 to 87.5%.

5.5.4. Titanomagnetite

Titanomagnetites are mostly composed of (70.6 – 79.6) iron, (7.7 – 20.7) TiO2 and minor amount of (0.72 – 3.47) MnO.

5.6. Amphibole

Amphiboles are an important group of minerals in a wide spectrum of igneous rocks from felsic to mafic end members. Further, they are major constituents in metamorphic rocks derived from basic igneous rocks and impure limestones.

Depending on Leake (1997), the amphiboles in the samples with formulas calculated on the basis of 23 of oxygens include: actinolite, richterite, magnesio-hornblende, actinolitic hornblende, and subsilicic gedrite.

Most of the amphiboles in the investigated rocks are calcic amphiboles; this group is characterized by (Ca + Na)$_B$ ≥ 1.34 and Na$_B$ < 0.67 (Table 6)

Si vs. Mg / (Mg+Fe) diagram after (Leake, 1997) is used to classify the calcic amphibole. This figure shows

Table 4. The chemical analyses of biotite and their formulae calculated on the basis of 22 oxygen.

Samples	Hc 1	X54 4	A9	X51 a
	Wt%	Wt%	Wt%	Wt%
SiO2	36.160	31.740	37.330	46.800
TiO2	2.490	2.370	2.080	0.050
Al2O3	17.070	16.190	14.640	35.260
Cr2O3	0.020	0.100	0.010	0.000
FeO	21.870	22.350	15.410	1.860
MnO	0.140	0.150	1.030	0.100
MgO	10.020	10.740	14.280	0.770
CaO	0.000	0.050	0.120	0.000
Na2O	0.240	0.180	0.120	0.520
K2O	7.930	5.940	8.560	10.570
BaO	0.110	0.130	0.170	0.060
TOTAL	96.050	89.940	93.750	95.990
Si	5.487	5.183	5.681	6.199
Al (iv)	2.513	2.817	2.319	1.801
T	8.000	8.000	8.000	8.000
Al (vi)	0.539	0.298	0.307	3.703
Ti	0.284	0.291	0.238	0.005
Cr	0.002	0.013	0.001	0.000
Fe(iii)	0.000	0.000	0.000	0.000
Fe(ii)	2.775	3.052	1.961	0.206
Mn	0.018	0.021	0.113	0.011
Mg	2.267	2.615	3.240	0.152
M	5.885	6.290	5.860	4.077
Ca	0.000	0.008	0.020	0.000
Na ***	0.071	0.057	0.035	0.134
K	1.535	1.237	1.662	1.786
Ba	0.007	0.008	0.010	0.003
I	1.613	1.310	1.727	1.923
X_{Mg}	31.421	32.457	48.097	29.278

that amphiboles are magnesio-hornblende and actinolites (Fig. 9).

The magnesium rich nature of the amphibole is reflected by its high Mg number (50% - 80 %). Si content ranges from (4.7 – 7.7 cation) but the majority of Si is less than 7.6. All the analyzed amphiboles contain sufficient Al to balance the Si deficiency in the tetrahedral sites.

The samples have low content of Na and K cations. The Na content in most of the samples ranges from 0.019 to 0.26 and K content ranges from .002 to 0.4. The studied samples have high Ca values, which reach 3.57 cation per
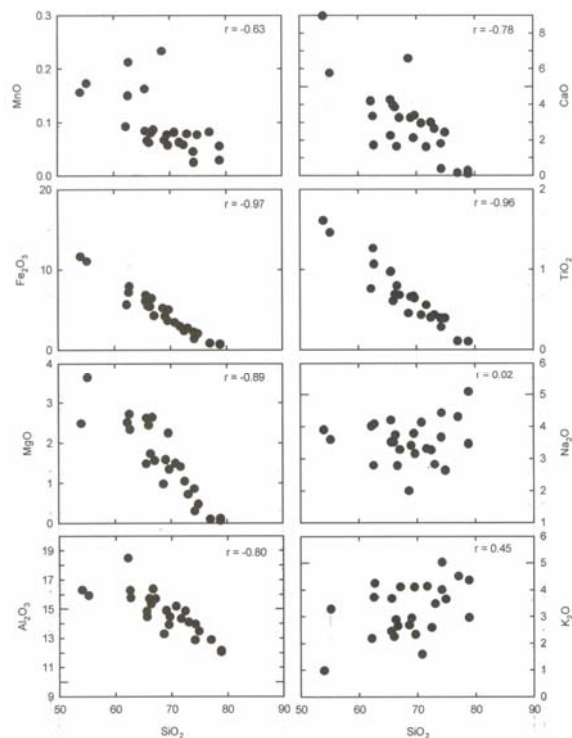

Figure 6 . Plots of SiO_2 vs. major elements for metaconglomerates. Note the positive correlation for SiO_2-K_2O, the scatter between SiO_2-Na_2O and negative correlation for SiO_2 and other major elements.
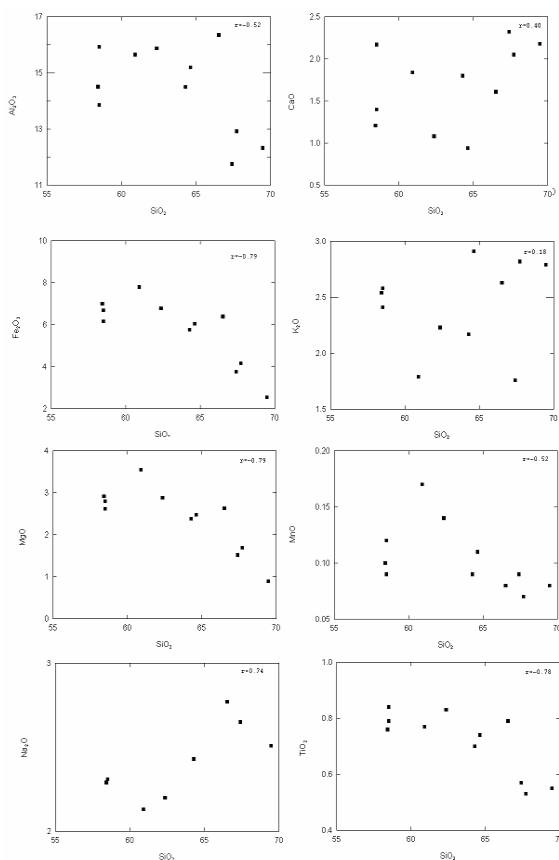

Figure 7. Plots of SiO_2 vs. major elements for hornfelses. Note the positive correlation for SiO_2 vs. K_2O, Na_2O and CaO and the negative correlation for SiO_2 and other major elements.

Table 5.a

Sample	54-X	54-X,	54-X	b-opaq	HC	b-	b-	HC
Na$_2$O	0.038	0.019	0.000	0.000	0.038	0.008	0.025	0.000
SiO$_2$	0.017	0.033	0.000	0.026	0.013	0.020	0.024	0.031
MgO	0.019	0.003	0.003	0.000	0.020	0.000	0.024	0.001
Al$_2$O$_3$	0.000	0.000	0.000	0.112	0.031	0.191	0.282	0.084
K$_2$O	0.023	0.039	0.000	0.000	0.020	0.000	0.008	0.013
CaO	0.030	0.066	0.155	0.064	0.198	0.079	0.079	0.248
FeO	46.261	39.112	35.215	91.957	79.626	92.083	90.894	84.095
TiO$_2$	47.396	51.046	51.218	0.408	7.702	0.170	0.305	6.157
Cr$_2$O$_3$	0.055	0.020	0.028	0.048	0.034	0.000	0.043	0.051
MnO	1.981	7.362	12.504	0.065	2.188	0.083	0.065	0.049
Sum	95.820	97.700	99.123	92.680	89.870	92.634	91.749	90.729
	Ilmenite	Ilmenite	Ilmenite	Magnetite	Titanomagnetite	Magnetite	Magnetite	Titanomagnetite

Table 5.b

Sample	H-II	H-II	H-II	Hc,	HC,
Na$_2$O	0.027	0.033	0.033	0.004	0.021
SiO$_2$	3.566	3.244	3.280	31.129	30.206
MgO	0.309	0.398	0.320	0.000	0.000
Al$_2$O$_3$	0.017	0.019	0.001	0.935	1.158
K$_2$O	0.000	0.025	0.000	0.000	0.002
CaO	0.304	0.296	0.196	28.118	26.682
FeO	75.592	75.232	73.095	1.349	1.888
TiO$_2$	0.012	0.003	0.088	38.097	35.924
Cr$_2$O$_3$	0.005	0.019	0.031	0.000	0.000
MnO	0.000	0.033	0.000	0.150	0.239
sum	79.832	79.302	77.044	99.782	96.120
	pyrite	Pyrite	pyrite	Titanite	Titanite

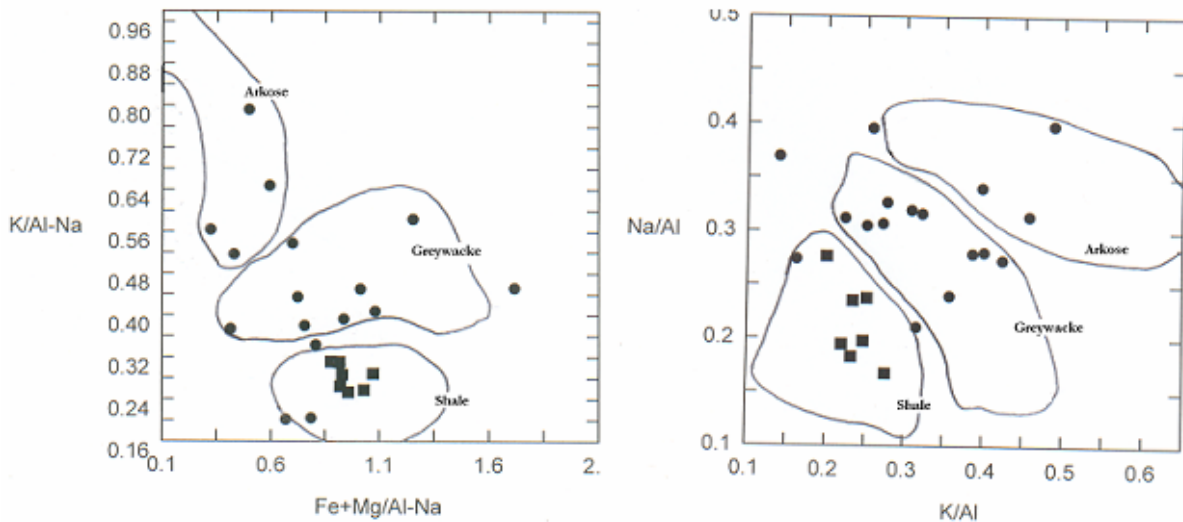Table 5 (a,b). The chemical data for titanite, sulphide, and oxides.

Figure 8. Plots of K/Al vs. Na/Al and (Fe+Mg)/(Al/Na) vs. K/(Al-Na) for the investigated rocks after (Saupe and Vegas, 1987). Note the hornfelses fall in shale field while the most of metaconglomerates fall in greywacke field and to lesser degree in arkoses field. The symbols as in (Fig. 6) and (Fig. 7).

unit formula. Table (6) shows the chemical formulas of selected amphiboles.

Table 6: The chemical analyses and formulae of amphibole.

Sample No.	A133	A1310	HC1	HC2
SiO_2	48.43	51.32	53.16	53.86
TiO_2	0.83	0.61	0.12	0.12
Al_2O_3	6.16	4.86	2.2	1.49
Cr_2O_3	0.04	0	0.01	0.02
FeO	15.29	13.53	8	6.46
MnO	0.43	0.53	1.33	1.15
MgO	12.56	14.2	14.34	14.52
CaO	11.98	12.14	20.6	23.84
Na_2O	0.74	0.46	0.43	0.41
K_2O	0.58	0.36	0.05	0.05
TOTAL	97.13	97.59	100.26	101.92
Si	7.186	7.435	7.444	7.393
Al^{iv}	0.814	0.565	0.363	0.241
T site	8	8	7.807	7.634
Al^{vi}	0.263	0.265	0	0
Cr	0.005	0	0.001	0.002
Fe^{3+}	0.026	0	0.595	0.741
Ti	0.093	0.067	0.013	0.012
Mg	2.778	3.066	2.993	0.134
Fe^{2+}	1.871	1.639	3.42	0
Mn	0.054	0.065	0.159	0.134
Ca	1.904	1.883	3.09	2.971
Na_b	0.006	0.015	0	0
Na_A	0.153	0.115	0.117	0.109
K	0.11	0.066	0.009	0.009

6. Geothermobarometry

Geothermometers are reactions that can be used to calculate or estimate temperature of formation of minerals (El shazly, 2001). The temperatures of equilibration applying the different calibrations (Powell & Powell (1977), Spencer & lindsley (1981), and   Andersen & lindsley (1985)) for some samples using the ILMAT excel sheet by LePage is given in Table (7).

The amphibole chemistry, in particular their Al and Na contents, can be used to evaluate the P – T conditions of metamorphism (Laird and Albee, 1981). During low temperature metamorphism the amphiboles tend to have low Al content relative to high temperature igneous amphiboles (Leak, 1971).

The Na in the (B site) and Al^{iv} content**s** in metamorphic amphiboles tends to increase as the metamorphic grade increases (Laird and Albee, 1981). Spear (1980) has used the exchange equilibria between plagioclase and hornblende (NaSi ↔ CaAl) to estimate the temperature of
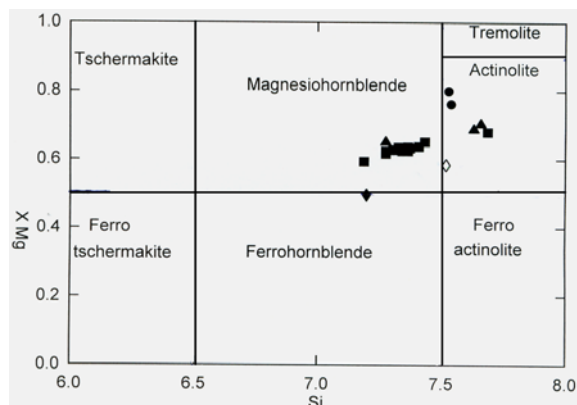

Figure 9. Mineral chemistry diagram of amphibole for the investigated rocks after (Leake, 1971). This figure is used to distinguish igneous from metamorphic amphiboles. Note that amphiboles fall exclusively in the metamorphic field. The symbols of samples are ■   represent A13 ▲   represent H II ◊ represent 6- int.
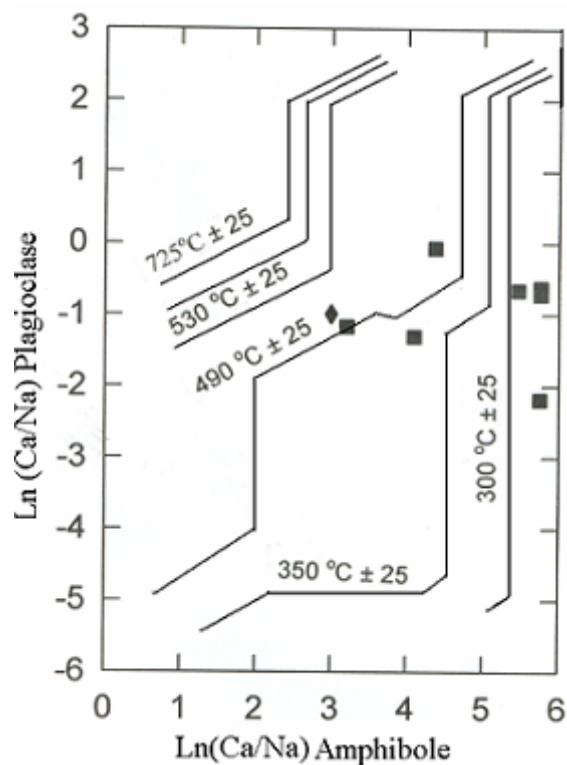

Figure10. ln (Ca/Na) $_{Amph.}$ – ln (Ca/Na) $_{plag.}$ diagram for the investigated rocks after (Spear, 1981). The hornfelses were formed at about 500^0C while the metaconglomerate were formed at temperatures   ◆ ween 490^0C to less than 300^0C. Symbols as in Fig. (9)   ▼ represent X54.

amphibole formation during metamorphism. The ln (Ca/Na) $_{plagioclase}$ vs. ln (Ca $_{B\ site}$ /Na $_{B\ site}$) $_{amphibole}$ diagram developed by Spear (1980) is used to estimate the temperature of metamorphism.

The data points plot close to the isotherms 490 ± 20 to 530 ± 20 °C and 300 ± 20 °C thus indicating a temperature of formation between 300 – 500 °C (Fig 10).

Figure 12 adopted from Leake (1971) shows that most amphibole samples have relatively low temperature amphiboles relative to high temperature igneous
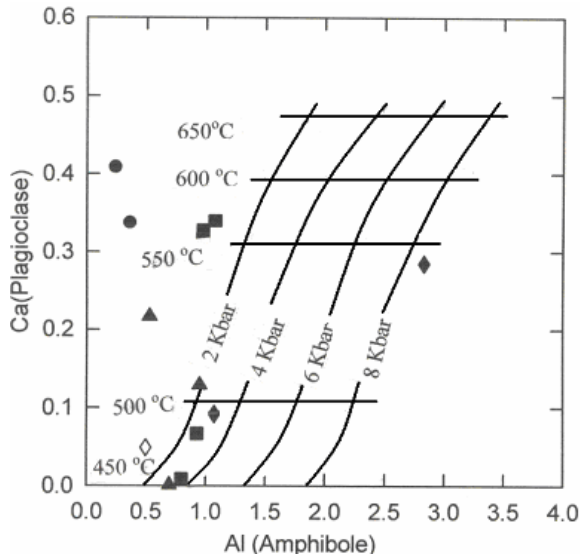
Figure 11. Al $_{amphibole}$ – Ca $_{plagioclase}$ diagram for the investigated rocks after (Plyusnina, 1982) is used to estimate the temperature and pressure of the metamorphic rocks. Note that metaconglomerates were formed at temperatures between 450^0C to about 610^0C and pressure less than 4Kbar, while the hornfelses were formed at 500^0C and pressures of less than 4 Kbar. Symbols as in Fig. (9) and Fig. (10) ● represent Hc.
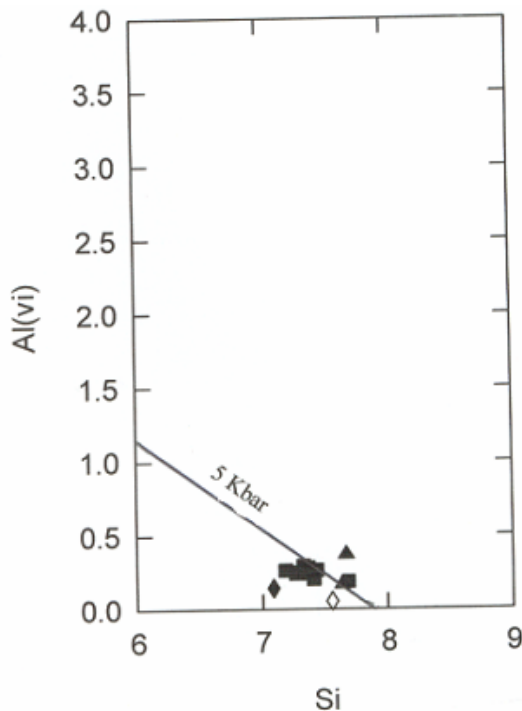

Figure 12. Al^{vi} – Si variation diagram for amphibole of the investigated rocks, after (Raase, 1974). Note that the majority of the amphiboles falls below the 5 Kbar curve. Symbols as in Fig. (9) and Fig. (10).

amphibole; this means these minerals were formed as a result of metamorphic processes.

Furthermore, Ca plagioclase vs. ∑ Al amphibole diagram (Fig 11) after (Plyusnina, 1982) is used to determine the temperature and pressure of metamorphic rocks. This diagram shows that the temperature of

Table 7. Geothermometric results obtained by three magnetite – ilmenite calibrations.

Sample no.	Average temp ^{o}C after Powell & Powell (1977)	Average temp ^{o}C after Spencer & lindsley (1981)	Average temp ^{o}C after Andersen & lindsley (1985)
b1	560	651	658
b2	333	468	463
HII1	370	492	490
HII2	308	437	428
HC	510	535	545

equilibration does not exceed 570 ^{0}C and the ranges between 450 to 610 ^{0}C, while the pressure does not exceed 4 Kbar with the exception of X54.

Amphiboles plot on the Al^{iv} vs. Si variation diagram (Raase, 1974) to the left of the 5- Kbar boundary or close to it (Fig 12).

7. Discussion and Conclusions

7.1. Economic Minerals (Sulfide Minerals)

Opaques are abundant in the metasediments and the intruded igneous dykes.

X- ray diffraction study has indicated that 12 out of 25 analyzed samples contain sulfide minerals (Fig 13). Pyrite, cinnabar, pyrrohtite, sphalerite, galena and chalcopyrite ferromagnesian silicates such as, biotite, amphibole, cordierite and chlorite in addition to garnet, staurolite are common constituents of silicate rocks that

host metamorphosed sulfides. These minerals become more magnesium with rich proximity to sulfide ore as a result of the effects of metamorphism and the increased fo2 and fs2 (Rosenberg, et al. 2000).

are distinguished as sulfides in the study area. However, the most widespread sulfides in the analyzed samples are chalcopyrite and pyrite.

Rosenberg, et al. (2000) has noticed that the samples with (>1 %) total sulfur shows a marked divergence between the iron content of the ferromagnesian mineral and the whole rock composition. This divergence reflects the sequestering of iron into sulfides, so that the ferromagnesian silicates have low X_{Fe} even though the rocks as a whole may be iron rich. This result agrees with the result of the analysis of biotite, pyroxene, and amphibole in the samples (A9, X51, X54, HC).

For example:

i) The X_{Fe} of biotite and pyroxene in A9 sample equals 51.9 and 44.6 respectively, while of the X_{Fe} of the whole rocks A9 equals to 84.1.

ii) X_{Fe} of biotite, pyroxene and amphibole of HC sample is 68.7, 28.2 and 36.2, respectively and X_{Fe} of the whole rock equals 73.38.

iii) X_{Fe} value of X51 sample equals 73.3 while the X_{Fe} of the whole rock equals 95.1.

The decrease of X_{Fe} of the ferromagnesian mineral especially of the biotite relative the whole rock results
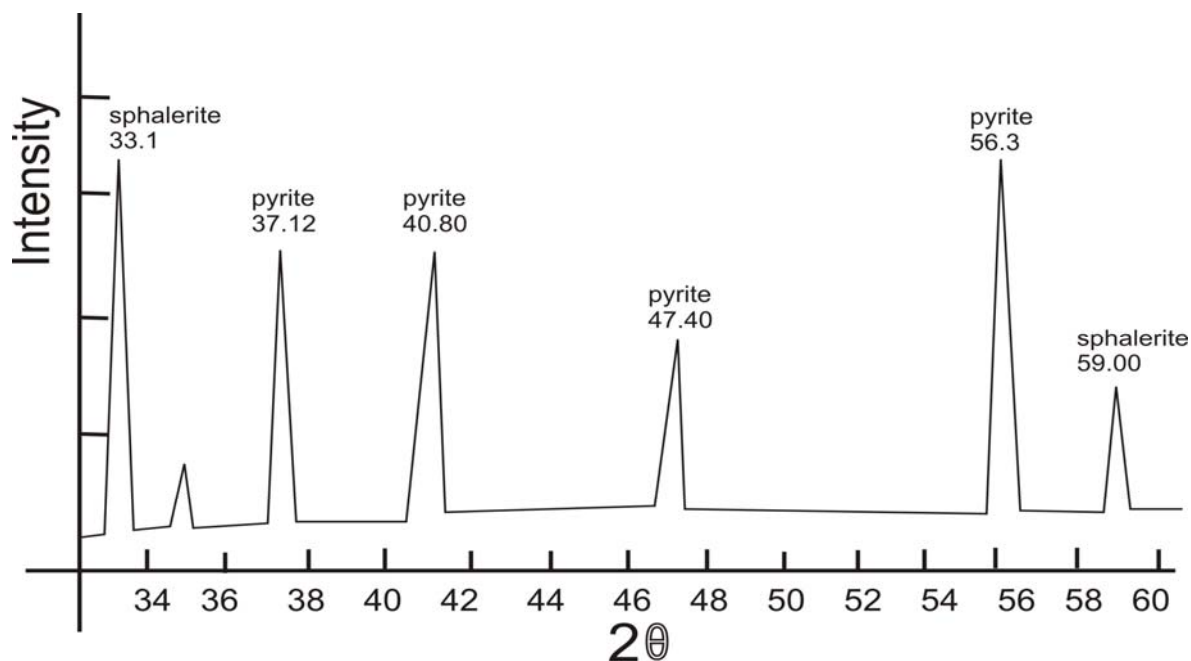
Figure 13. XRD pattern of metaconglomerates sample contain some of sulphide minerals.

from the increase of $f\mathrm{O}_2$. The increase of oxygen fugacity is elevated; the iron in this mineral is oxidized into ferric state.

The Fe^{+3} cannot enter most Fe^{+2} – Mg silicate of metamorphic rocks such as biotite and cordierite, (Hyndman, 1985), therefore the $\mathrm{X_{Fe}}$ of ferromagnesian minerals becomes lower than XFe of the whole rocks.

Sample X51 has $\mathrm{Fe_2O_3}$ (Fe^{+3}) of 38.3 and FeO (Fe^{+2}) of 22.4. The high value of Fe^{+3} reflects the high fo2 and the enrichment with sulfide minerals. This result agrees with the hand specimen inspection and the mineral chemistry.

Larsen et al. (1995) have noticed that the biotite in rocks in and immediately adjacent to sulfide ore are enriched in fluorine; and biotite rich in fluorine tends to have low iron content due to Fe – F avoidance (Rosenberg et al., 2000)

A9, X51 and HC samples have relatively high fluorine values of 0.94, 0.25 and 0.095% respectively.

On the basis of the above observations, it is suggested that the opaque minerals in the study area are discouraging to consider them of economic value.

7.2. Geothermobarometry

7.2.1. Hornfelses

The plagioclase in the hornfelses has an oligoclase and andesine composition. It becomes more calcic and changes from albite in greenschist facies to oligoclase in epidote amphibolite facies (Barker, 1990). The low temperature limit of amphibolite facies is set by appearance of oligoclase (Hyndman, 1985).
Some samples contain sillimanite and do not contain cordierite. Sillimanite in these samples could be the result of the reaction:
Garnet   + cordierite   = biotite   + sillimanite (Katz et al. 1998).
The mineral content and the temperature and pressure of formation of the analyzed samples confirm their

occurrence in the amphibolite facies close to the contact with the intruded granite.

7.2.2. Metaconglomerate

The amphiboles in metaconglomerates samples are actinolite, actinolitic hornblende and magnesian hornblende. Actinolite is a characteristic mineral of the greenschist facies (Klein , 2002). Prograde metamorphism changes amphibole composition from actinolite to hornblende (Laird and Albee, 1981). Plagioclase also becomes more calcic with increasing the metamorphic grade and the presence of oligoclase characterizes the epidote amphibolite facies. (Barker, 1990)

Plagioclases in A13 and HC are of andesine composition, and in other samples as indicated by the X-ray diffraction results into oligoclase, albite and labradorite.

The different types of plagioclase minerals in the same samples reflect the different origin of rocks. Diopside also exists in sample HC and was identified by microscope and X- ray in some other samples. Barker (1990) suggested that the coexistence of tremolite and diopside is characteristic of temperatures of the order 500–650 ºC. Depending on the pressure and temperature of formation, texture, mineralogical composition, and chemical data, metamorphism belongs to a greenschist to amphibolite facies

8. Acknowledgements

References

[1] Barker, A. J., 1990. Introduction to metamorphic textures and microstructures. 1st Ed., Blackie and Sons, London.

[2] El-Shazly, A. K., 2001. Are pressures for blueschists and eclogites overestimated? The case from NE Oman, *Lithos, 56: 231-264.*

[3] Gu, X. X., Liu, J. M., Zheng, J. H., Tang, J.X., and Qi, L., 2002. Provenance and tectonic setting of the Proterozoic turbidites in Hunan, south China: geochemical evidence. *Journal of sedimentary Research, 3 (72): 393-407.*

[4] Hassuneh, M. 1994. Geological, Petrological and geochemical investigation of the Janub metamorphic suite rocks in Wadi Es-Sabil, Ain El-Hasheem area, SE Aqaba. *Unpubl. M. Sc. Thesis, University of Jordan.*

[5] Hyndman, D.W. 1985. Petrology of igneous and metamorphic rocks. 2nd Ed., McGraw-Hill Book Company, New York.

[6] Jarrar, G., Stern, R. J., Saffarini, G., and Al-Zubi, H., 2003. Late-and post-orogenic Neoprotrezoic intrusions of Jordan: implication for crustal growth in the northernmost segment of the East African Orogen, *Precambrian Research, 123: 295-319.*

[7] Katz, O., Avigad, D., Matthews, A., and Heimann, A., 1998. Precambrian metamorphic evolution of the Arabian-Nubian Shield in the Roded area, southern Israel, *Israel Journal of Earth Science, 47: 93-110.*

[8] Klein, C. 2002. The Manual of Mineral Science. 22nd Ed. John Wiley and Sons, New York.

[9] Kröner, A., 1985. Ophiolites, and the evolution of tectonic boundaries in the late Proterozoic Arabian- Nubian Shield of Northeast Africa and Arabia, Precambrian *Research, 27: 235-257.*

[10] Laird, J., and Albee, A.L., 1981. Pressure, temperature and time indicators in mafic schist: their application to reconstructing the polymetamorphic history of Vermont, *American Journal of Science, 281: 127-175.*

[11] Larsen, R. B., Walker, N., Birkeland, A., and Bjerkgad, T., 1995. Fluorine-rich biotite and alkali- metasomatism as guides to massive sulfide deposits: an example from the Bleikvassli Zn-Pb- (Cu) deposit, Norway. *From http: www.the-conference.com/ jCon fAbs/1/350.html*

[12] Leake, B. N., 1971. On aluminous and edenitic hornblendes, Mineralogical *Magazine, 38: 389-407.*

[13] Leake, B. N., 1997. Nomenclature of Amphiboles; Report of the Subcommittee on Amphiboles of the international Mineralogical Association Commission of new Minerals and mineral names, *European Journal of Mineralogy, 9: 623-651.*

[14] McCourt, W. J., Ibrahim, K. M., 1990. The geology, geochemistry and tectonic setting of the granitic and associated rocks in the Aqapa and Araba complexes of southwest Jordan, *Bulletin Geological Mapping Division 10, Natural Resources Authority, Jordan.*

[15] Morimoto, N., 1988. Nomenclature of pyroxenes, *American Mineralogist, 73: 1123-1133.*

[16] Naqvi, S.M., Sawkar, R.H., Subba Rao, D.V., Govil, P.K. and Gnaneswar Rao, T., 1988. Geology, Geochemistry and tectonic setting of Archaean greywackes from Karnataka Nucleus, India, Precambrian *research, 39: 193-216.*

[17] Plyusnina, L. P., 1982. Geothermometry and geobarometry of plagioclase- hornblende bearing assemblages, *Contributions to Mineralogy and Petrology, 80: 140-147.*

[18] Raase, P., 1974. Al and Ti contents of hornblende, indicators of pressure and temperature of regional metamorphism, *Contributions to Mineralogy and Petrology, 45: 231-236.*

[19] Rabb'a, I., and Ibrahim, K. M. (1988). Petrography of the plutonic rocks of the Aqaba Complex, *Bulletin Geological Mapping Division 9, Natural Resources Authority, Jordan.*

[20] Rosenberg, J. L, Spry, P. G., and Jacobson, C. E., 2000. The effects of sulfidation and oxidation during metamorphism on composit- ionally varied rocks adjacent to the Bleikvassli Zn-Pb- (Cu) deposit, Nordland, Norway, *Mineralium Deposita, 35: 714-726.*

[21] Saupe, F., and Vegas, G., 1987. Chemical and mineralogical compositions of black shale middle Paleozoic of the central Pyrenees, Haute-Garonne, France, *Mineralogical Magazine, 51: 357-369.*

[22] Spear, F. S., 1980. NaSi-CaAl exchange equilibrium between plagioclase and amphibole: An empirical model, *Contributions to Mineralogy and Petrology, 72: 33-44.*

[23] Wones, D. R., and Eugster, H. P., 1965. Stability of biotite: experimental, theory and application, *Geological Society of London, 50: 1228-1272.*

[24] Yardly, B. w. 1989. An introduction to metamorphic petrology. 2nd Ed., Longman, Edinburgh.

[25] Zachmann, D. W., 1988. Matrix effects in separation of Rare-Earth Elements, scandium, and yttrium and their determination by inductively coupled plasma optical emission spectroscopy, *Analytical Chemistry, 60: 420-7.*